# Optimizing the performance of CPML optical target for light-scattering simulations

**Sergio Cantero and Snow H. Tseng***

*Graduate Institute of Photonics and Optoelectronics, National Taiwan University, Taipei 10617, Taiwan*
**Corresponding author: stseng@ntu.edu.tw*

Received January 7, 2015; revised February 15, 2015; accepted February 17, 2015;
posted February 18, 2015 (Doc. ID 231805); published March 17, 2015

An optical target constructed by modifying the convolutional perfectly matched layers (CPML) formulation is tested for applications in light-scattering simulations. The optical target is designed for finite-difference time-domain light-scattering simulations to eliminate and isolate impinging light. The performance of the optical target under different incident light and factors affecting the absorption efficiency is analyzed. Variations of the optical target geometry are tested for optimal absorption. Simulation results show that the absorption is most effective for normally impinging light; its absorption cross section can be effectively tuned by modifying the layers' conductivity profile. In scattering simulations, the performance of such absorbing medium can effectively absorb incident light from arbitrary directions within a light-scattering simulation. 

*OCIS codes:* (290.4210) Multiple scattering; (050.1755) Computational electromagnetic methods.
http://dx.doi.org/10.1364/JOSAB.32.000628

## 1. INTRODUCTION

Biomedical optics is generally limited by the scattering effect of a macroscopic scattering medium such as biological tissue structures. The propagation of light is randomized by irregular geometry. The performance of biomedical optics can be significantly enhanced if light can be directed through a scattering medium to a target position accurately through a macroscopic scattering medium, i.e., biological tissue structures.

In the past decade, simulation methods such as the finite-difference time-domain (FDTD) technique have enabled accurate modeling of light propagation through a macroscopic scattering medium; such simulations can provide important information for the development of biomedical imaging techniques [1]. Based on numerical solutions of Maxwell's equations, the FDTD algorithm is a robust computational method that can accurately account for the wave nature of light. The optical characteristics of biological structures can be modeled using the FDTD simulation. The FDTD simulation technique yields electromagnetic field information such as the amplitude and phase of light. Such simulation models can be used to enhance the understanding of various optical phenomenon such as optical phase conjugation (OPC) [2] or the time-reversed ultrasound-encoded light technique [3], which involves propagating light through a macroscopic scattering medium to a specific position. An accurate simulation of light propagation through a turbid medium such as biological tissue is becoming increasingly feasible; thus, it can provide essential information of the electromagnetic field in the research of biomedical optics.

Recently, macroscopic random media has been exploited to enhance light focusing. Research reported includes using layers of scattering medium to achieve subdiffraction limited focusing [4], pulse compression [5], or delivering light into a turbid media [6]. Due to the complexity of macroscopic, irregular geometry and inhomogeneity of biological tissues, numerical modeling is essential to achieve a better understanding of light propagation through such turbid media. To model light propagation through a turbid medium, a numerical optical target that can effectively eliminate impinging light at a specific position without distorting the neighboring electromagnetic field is required (Fig. 1); thus, a simulation of a plane wave impinging upon an optical target embedded within a macroscopic scattering medium. By eliminating the impinging light, the optical target can be used to analyze an electromagnetic field at a specific location within a light scattering simulation.

Previous research reported the possibility to implement an optical absorber within an FDTD simulation grid that can approximately eliminate light impinging from all directions [7]. This optical target is constructed by modifying the convolutional perfectly matched layers' (CPML) absorbing boundary condition (ABC) planar morphology into a round-shape absorber [8]. In this article, we further analyze the distribution of numerical error in the process of eliminating the impinging light by the CPML target. Quantitative analysis of the absorption performance is discussed in detail. Furthermore, instead of a conventional layered structure, we report an optimal CPML with each grid point assigned a specific conductivity; thus, the performance of the reported CPML target that surpasses the performance of the initially proposed CPML absorber [7,8]. Our goal is to optimize the performance of the CPML optical target to eliminate impinging light from arbitrary directions.

A review of the CPML method and theoretical construct is presented in Section 2. A detailed analysis of how the shaping of the optical target affects the absorption performance and measurements of the angular dependency of scattering errors is described in Section 3. Last, a summary for optimal implementation of the CPML optical target is presented in Section 4.

 

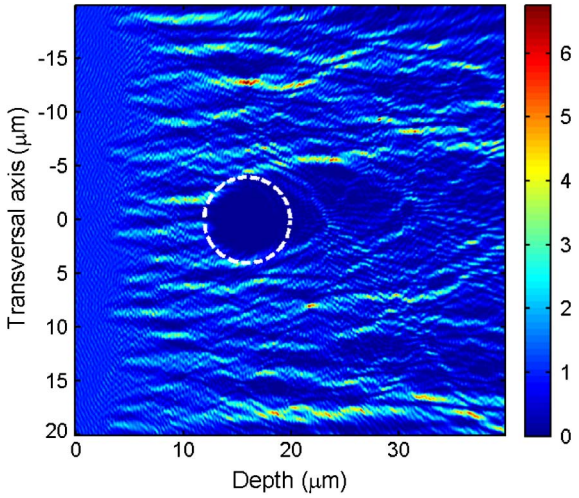


Fig. 1. Plane wave impinges upon an optical target and is partially absorbed within a scattering medium.

## 2. NUMERICAL MODEL

An optical target that can eliminate impinging waves from arbitrary directions is needed for simulations of light propagation through a macroscopic scattering medium. Several approaches to construct an omnidirectional electromagnetic absorber have been proposed [9,10]. These applications benefit from the possibility to either guide incident waves to an inner core or efficiently absorb the incident light. With the purpose of fabricating a nearly perfect absorbing medium, the first approach consisted of using a nonmagnetic isotropic media. However, though easy to fabricate, these media are not reflectionless (impedance-matched) and require a low permittivity gradient or, equivalently, a large thickness to produce low reflections.

An ideal optical target that can absorb impinging light without reverberation is proposed [7]. To construct such an optical target, we modify the perfectly matched layers' (PML) [11] ABC to construct a near-reflectionless absorber [12]. However, to employ the PML algorithm on a convex surface as an optical target is numerically unstable [13,14]. Instead of using a convex metric for the PML on a curved surface, we use the planar PML metric and construct a circular optical target made of convex layers of such a PML medium. Although not perfectly matched in the continuum limit [12], such type of absorber can nevertheless yield very good performance. Note that another source of spurious reflections is the stair-casing error of the numerical grid, which can be easily minimized by using small grid cells. Conductivity mismatch between impedance-matched layers do not occur exclusively along the direction matched to the spatial metric, as in PML ABC, but in every direction, due to this spatial sampling of the circular optical target.

The proposed optical target is implemented in the FDTD algorithm by modifying the CPML ABC formulation by Roden and Gedney [15]. This formulation has the advantage of being independent of the background medium. This separate implementation allows the construction of the optical target in different FDTD formulations as well as variations such as the pseudospectral time-domain technique [16]. In addition, in large-scale simulations it is not necessary to store additional variables for the optical target in the entirety of the region but exclusively at the region occupied by the absorber. The increase in computation time by implementing the proposed method is, therefore, low in comparison to the total computation time.

Within the FDTD loop, the recursive convolution is iteratively stored in the auxiliary function, $\Psi$, which is separately updated at each time step. The corresponding field component is then linearly adjusted by this function. After computing the field components, every iteration utilizing the discrete form of Maxwell equations [17], the adjustment of each field component at the CPML region is in the form

$$E_z|_{i,j}^{n+\frac{1}{2}} = [E_z|_{i,j}^{n+\frac{1}{2}}]_{\text{Maxwell Eq.}} + C_b\{\Psi_{E_{z,x}|_{i,j}^{n}} - \Psi_{E_{x,y}|_{i,j}^{n}}\}. \quad (1)$$

Similar equations are used for the other TM mode components. Here, Cb is the updated coefficient in FDTD equations corresponding to the background medium where the CPML region is placed. For a lossless medium, Cb becomes simply $\Delta t/\varepsilon\Delta$. The function $\Psi$ is updated together at every time step via

$$\Psi_{E_{z,x}|_{i,j}^{n}} = \Psi_{E_{z,x}|_{i,j}^{n-1}} + c_{i,j}\left(\frac{H_y|_{i+\frac{1}{2},j}^{n} - H_y|_{i-\frac{1}{2},j}^{n}}{\Delta x}\right), \quad (2)$$

where the $b$ and $c$ coefficients are given by

$$c_{i,j} = \frac{\sigma_{i,j}}{\sigma_{i,j}\kappa_{i,j} + \kappa_{i,j}^2\alpha_{i,j}}\left[e^{-\left(\frac{\sigma_{i,j}}{\varepsilon_0\kappa_{i,j}} + \frac{\alpha_{i,j}}{\varepsilon_0}\right)\Delta t} - 1\right], \quad (3)$$

$$b_{i,j} = e^{-\left(\frac{\sigma_{i,j}}{\varepsilon_0\kappa_{i,j}} + \frac{\alpha_{i,j}}{\varepsilon_0}\right)\Delta t}. \quad (4)$$

Further discussion of these parameters and the central-frequency-shift tensor can be found in [18]. Since plane waves with a narrow bandwidth are typically used in FDTD simulations, no special control of the frequency behavior of the CPML is necessary, and the parameters $\alpha$ and $\kappa$ can be set to 0 and 1, respectively. The use of an optical target under different situations may require different values of these two parameters for better performance.

In order for effective absorption of impinging fields from all directions, the electric and magnetic conductivities are assigned with values tapering down from the center:

$$\begin{cases} \sigma(x,y,z) = \sigma_0\left(\frac{L_{\max} - L(x,y,z)}{L_{\max}}\right)^m \\ \sigma_0 = 0.8\frac{m+1}{\eta\Delta} \end{cases}. \quad (5)$$

Each node $(x,y,z)$ of the FDTD grid is associated to a certain layer, with index $L$, so that the nodes at every layer are considered at the same distance from the center. Although $L$ varies, depending on the morphology of the CPML region, $L_{\max}$ corresponds to the number of layers in the CPML construct. $L(r)$ equals to $L_{\max}$ at the interface with the rest of the simulation region; thus, the inner boundary of the CPML is considered the absorbing boundary condition or outer boundary if placed within the simulation. In Eq. (5), $\Delta$ denotes the grid size and $\eta$ the wave impedance. A smaller grid size

$\Delta$ can be chosen to reduce the stair-casing error. For circular geometry, $L_{\max}$ is simply the radius of the CPML region, and $L(r)$ is the distance from the layer assigned to a grid point $(x, y, z)$ to the outer boundary. Although smaller optical targets are highly affected by the layer and grid-different morphology, the limit $r$ approaching infinity is equivalent to planar PML.

The initial attempt to test the viability of the optical target under omnidirectional light absorption has been reported in [7]. Here, we further analyze the performance of the possibility of employing the optical target within scattering simulations, i.e., for applications in simulations of biomedical optical techniques. Under this setup, light propagation is not omnidirectional but highly scattered in strongly focused optical paths [19]. In addition, it is important to identify the directionality and possible peaks of the distribution of numerical errors. A different approach is, therefore, required.

## 3. RESULTS

### A. Overall Absorption

To test the overall efficiency, the absorption of a circular converging wavefront is compared to the PML ABC. As shown in Fig. 2, the error as a function of the size of the target with constant layer resolutions is presented. Here, a circular wavefront impinges upon the optical target in the radial direction, which is analogous to a plane wave impinging upon a CPML ABC. Results from this simulation show that, with an increased radius of the optical target, the amount of absorbed light is similar to the CPML ABC, as expected. The accuracy of the CPML optical target is, therefore, determined by the size of the optical target and the grid resolution of the simulation.

To ensure complete sampling of the temporal and spatial frequencies, the total computational region spans $1000 \times 1000$ grid points ($32\ \mu m \times 32\ \mu m$); the simulation region is surrounded by a 20-layer CPML ABC to eliminate reflection caused by the outgoing waves. With a central wavelength $\lambda_0 = 632.8$ nm, the spatial resolution is chosen to be $\lambda_0/20$, corresponding to physical spacing between grid points of 31.64 nm, which is small enough to minimize the numerical dispersion anisotropy without requiring the use of very large grids and computation time. The computational time of a single simulation is approximately 30 min with a single Intel processor.

For a grid-based simulation, in which parameters are assigned only at the grid points, it is possible to assign $\sigma$ and $m$ with a finer resolution beyond 40 layers per wavelength, thus assigning the parameters $\sigma$ and $m$ as a function of distance from the center of the optical target staggered according to the grid points. Minimal reflection is achieved when every grid point is assigned a different conductivity value.

### B. Directional Light Absorption

For light propagation in a macroscopic scattering medium, the direction of incident light is generally arbitrary due to scattering of the irregular geometry. To analyze the optical target performance, we analyze the absorption using a focused Gaussian beam. A schematic of the proposed numerical experiment is shown in Fig. 3. The optical target in this setup is designed to absorb incident light from a specific direction.

A light pulse with a Gaussian cross-sectional profile and a Gaussian temporal waveform is implemented as a soft source [17]. Using a broadband pulse instead of a continuous-wave (CW) single frequency permits observing a range of incident wavelengths. The temporal width is restrained in the lower limit by the numerical errors due to temporal sampling and in the higher limit by the requirement to fit the entire pulse within the region during the measurement time interval. The temporal FWHM of the light source varies from 141 to 500 temporal iterations. From the Courant stability criterion, the time stepping is limited to $\Delta t \le \Delta/(c\sqrt{2}) \approx 0.0748$ fs for a resolution of 31.6 nm. The corresponding FWHM values range from 10.5 to 37.4 fs.

A Gaussian pulse impinging upon an optical target is shown in Fig. 3. The electric field amplitude is depicted to show the elimination of the impinging field. In Fig. 3(a), the pulsed Gaussian beam approaches the optical target; (b) it impinges upon the surface of the optical target; (c) the wavefront is scattered by the optical target; and (d) incident energy is nearly completely eliminated by the optical target. Due to

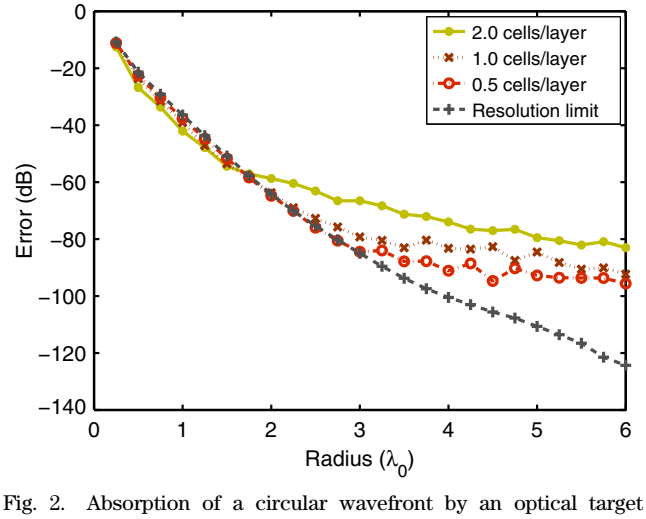


Fig. 2. Absorption of a circular wavefront by an optical target with radius ranging from 158 to 3797 nm. The resolution limit corresponds to an absorber with each point in the grid assigned a different conductivity.

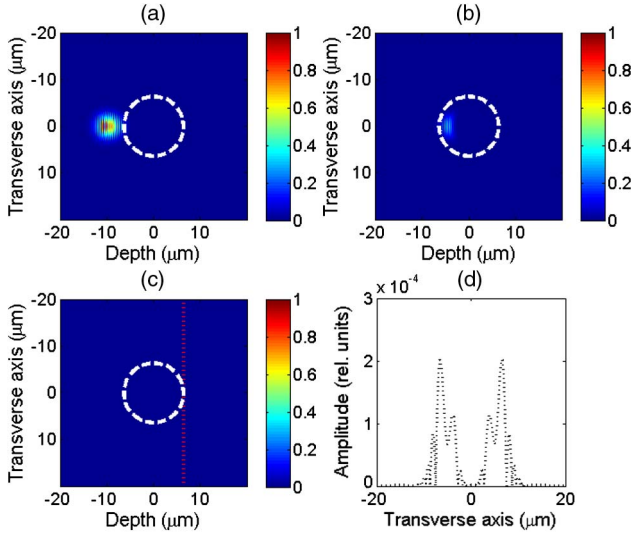


Fig. 3. Absorption of a Gaussian beam with pulsed temporal profile by the optical target at (a) 60 fs; (b) 72 fs; and (c) 85 fs. (d) Profile of the electric field amplitude in (c) at the red dotted line.

imperfect elimination, a minimal residual field emerges. As shown in Fig. 3(d), the maximum field amplitude in Figs. 3(c) and 3(d) is four orders of magnitude lower than the incident field, demonstrating that the optical target can effectively absorb an incident Gaussian beam.

Absorption error is not homogeneous: light is mostly absorbed at the center, and residual light emerges from the side. The reduction of electric and magnetic conductivities (and therefore losses) along the paths farther from the optical axis is the main cause of this residual light. Furthermore, the angle between the wavefront and the target boundary progressively increases with misaligned incident wave relative to the CPML parameter gradient, resulting in increased residual scattered light. For a Gaussian beam impinging upon an optical target, optimal performance is achieved when the central axis of the Gaussian beam is normal to the optical target.

### C. Scattering of Residual Light

To test the performance of a circular optical target, we compare the scattering of numerical errors in the near field of the optical target, to a rectangular PML absorber. The numerical error introduced in the near field of the optical target is obtained by comparing it to the ideal case, i.e., zero reflection: the electromagnetic field recorded at a set of points equally distant from the target center. The maximum error distribution is calculated and plotted as a function of the angle to illustrate the dependence of directionality (Fig. 4).

As shown in Fig. 4, the field amplitude scattered in the forward direction is slightly reduced relative to the incident light. The distribution of the remaining field from a small optical target corresponds to more forward and less backward reflections. Absorption increases with the size, with an evident directionality of the remaining field, presenting larger transmission than reflection. It is observed that the limit for larger sizes becomes similar to the performance of a planar PML: For an optical target with a radius of 3.16 μm, the residual field drops down to −150 dB.

The maximum error of the planar CPML for a different tilt angle is shown in Fig. 5, with the circular case (dashed line) as reference. The scattered energy of a planar optical target with no tilt (black line) is lower than the circular target (red line). In this case, the Gaussian beam impinges the planar optical

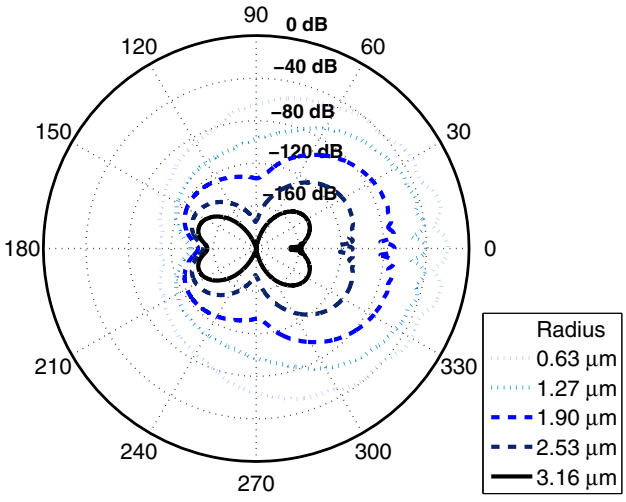


Fig. 4. Scattered field from a circular optical target of different sizes. Incident beam waist is 1.27 μm.

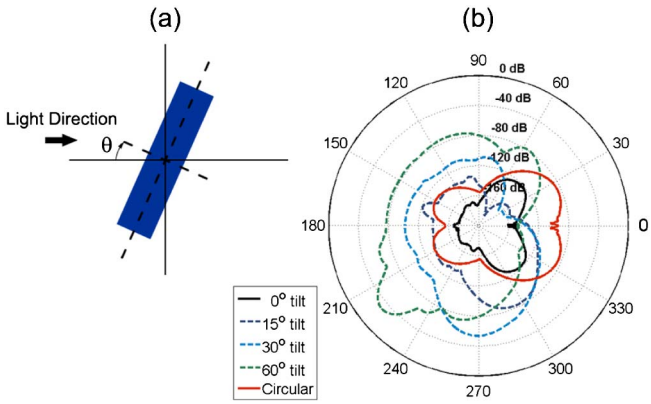


Fig. 5. Scattered field from a circular versus planar optical target with different tilt angles. (a) Schematics of the numerical setup. (b) Angular distribution of the scattered field compared to the circular target.

target at normal incidence, similar to a plane wave eliminated by a conventional CPML absorbing boundary condition (as implemented at the outer edge of an FDTD simulation grid), resulting in minimal error.

The performance of the circular optical target is invariant with respect to the angle of incidence, whereas the planar target is designed to absorb impinging light at normal incidence. As shown in Fig. 5, with a tilt angle ($\theta$) between the wavefront and the planar optical target, more residual light emerges and scatters into various directions. As the tilt angle is increased beyond 15 deg, the maximum error of a tilted rectangular optical target becomes larger than the error of a circular target.

In a situation where the absorber is placed inside a medium with an unknown incident source, a portion of the energy may propagate along the outer layers of the optical target. In this case, as shown in Fig. 3, some energy is transmitted back to the problem region. One way to reduce this undesired scattering is to design a steeper conductivity profile. To prevent higher reflections from the inner regions in the absorber, the maximum is not at the center but at a distance $r_{in}$ from the center. This is equivalent to wrapping a planar CPML around a hollow center. For a homogeneous incident light intensity along the transversal cross section of the target, the light source modeled in this setup is a CW plane wave with constant amplitude along the wavefront. The transversal section of the electric amplitude at the center of the optical target is stored and presented in Fig. 6 for varying thickness of the CPML absorbing layer in the optical target.

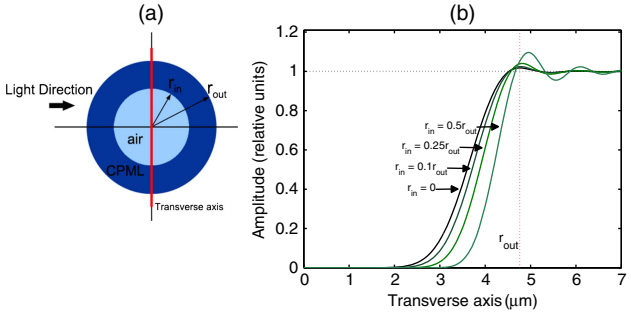


Fig. 6. Scattered field from a circular and planar optical target with different tilt angles. (a) Schematics of the numerical setup. (b) Angular distribution of the scattered field compared to the circular target.

In Fig. 6, as the thickness of the CPML region is decreased, the effective absorption radius is increased; as a result, higher leakage occurs at the boundary of the target (red dashed line). The electromagnetic energy propagating parallel to the layers is not completely absorbed by the CPML region. A thin CPML with few layers causes large overshoots. However, if the incident light does not cover the entire cross section of the optical target, the portion of light effectively absorbed is increased. While a CPML covering the entire cylinder produces the least residual scattered light for omnidirectional incidence, reducing its thickness can control the efficiency in which directional light incidence is absorbed. In summary, the conditions of the problem where the optical target is placed determine its appropriate morphology for optimal extraction of the electromagnetic energy.

## 4. CONCLUSION

The CPML algorithm was designed to absorb impinging light most effectively for normal incidence. Due to the adaptation of a planar geometry CPML to a circular geometry, simulations show that numerical error varies depending on the specific morphology of the source, the grid, and the geometry of the absorbing medium. By matching the optical target boundary with direction of the impinging light, the absorption can be optimized. However, in problems where the geometry of the incident energy is unknown or inhomogeneous, a circular target is easier to implement; the symmetrical geometry of the optical target allows it to reduce overall reflections for light impinging from an arbitrary angle. The simulations reported in this article demonstrate that the proposed circular optical target is suitable for absorbing light for different incidence angles.

For a circular optical target, the absorption error of the impinging circular waves and Gaussian beam is on the order of −80 dB or below. Absorption of the circular optical target is not perfect, due to the adaptation of the constitutive parameters of a CPML absorber, which was originally designed for planar geometry. Error analysis shows that the performance of the optical target is comparable to the CPML ABC typically implemented at the outer edge of a simulation. Although absorption is not homogeneous across the optical target, and larger leakage occurs at the edges, controlling the conductivity gradient can increase the effective absorption cross section of the optical target. In general, the error is low enough for general light-scattering simulations.

For large-scale simulations of light propagation through a turbid medium (e.g., biological tissue structure), an optical target to absorb incident light without distortion of the surrounding electromagnetic field is required to enable quantitative analysis of light propagated to the target position. Furthermore, an ideal absorbing numerical construct can be used to simulate a tracking object for detection and diagnosis purposes. Such simulations can shed new light on the understanding and development of light propagation through turbid media, which is essential to all biomedical optical techniques.

## REFERENCES


1. V. Ntziachristos, “Going deeper than microscopy: the optical imaging frontier in biology,” Nat. Methods **7**, 603–614 (2010).
2. S. H. Tseng and C. Yang, “2-D PSTD Simulation of optical phase conjugation for turbidity suppression,” Opt. Express **15**, 16005–16016 (2007).
3. Y. M. Wang, B. Judkewitz, C. A. DiMarzio, and C. Yang, “Deep-tissue focal fluorescence imaging with digitally time-reversed ultrasound-encoded light,” Nat. Commun. **3**, 928 (2012).
4. J.-H. Park, C. Park, H. Yu, J. Park, S. Han, J. Shin, S. H. Ko, K. T. Nam, Y.-H. Cho, and Y. Park, “Subwavelength light focusing using random nanoparticles,” Nat. Photonics **7**, 454–458 (2013).
5. O. Katz, E. Small, Y. Bromberg, and Y. Silberberg, “Focusing and compression of ultrashort pulses through scattering media,” Nat. Photonics **5**, 372–377 (2011).
6. J. L. Hollmann, R. Horstmeyer, C. Yang, and C. A. DiMarzio, “Analysis and modeling of an ultrasound-modulated guide star to increase the depth of focusing in a turbid medium,” J. Biomed. Opt. **18**, 025004 (2013).
7. S. Cantero, Y. Huang, and S. H. Tseng, “FDTD simulation of an optical absorber based on CPML absorbing boundary condition,” Proc. SPIE **8952**, 89520–89528 (2014).
8. Y.-A. Huang, Y.-T. Hung, and S. H. Tseng, “An optical target to eliminate impinging light in a light scattering simulation,” Comput. Phys. Commun. **185**, 2504–2509 (2014).
9. C. Argyropoulos, E. Kallos, and Y. Hao, “FDTD analysis of the optical black hole,” J. Opt. Soc. Amer. B **27**, 2020–2025 (2010).
10. E. E. Narimanov and A. V. Kildishev, “Optical black hole: Broadband omnidirectional light absorber,” Appl. Phys. Lett. **95**, 041106 (2009).
11. J.-P. Berenger, “A perfectly matched layer for the absorption of electromagnetic waves,” J. Comput. Phys. **114**, 185–200 (1994).
12. H. Odabasi, F. L. Teixeira, and W. C. Chew, “Impedance-matched absorbers and optical pseudo black holes,” J. Opt. Soc. Amer. B **28**, 1317–1323 (2011).
13. F. L. Teixeira, K. P. Hwang, W. C. Chew, and J. M. Jin, “Conformal PML-FDTD schemes for electromagnetic field simulations: a dynamic stability study,” IEEE Trans. Microwave Theory Tech. **49**, 902–912 (2001).
14. F. L. Teixeira and W. C. Chew, “On causality and dynamic stability of perfectly matched layers for FDTD simulations,” IEEE Trans. Microwave Theory Tech. **47**, 775–785 (1999).
15. J. A. Roden and S. D. Gedney, “Convolution PML (CPML): An efficient FDTD implementation of the CFS-PML for arbitrary media,” Microw. Opt. Tech. Lett. **27**, 334–339 (2000).
16. Q.-H. Liu, “Large-scale simulations of electromagnetic and acoustic measurements using the pseudospectral time-domain (PSTD) algorithm,” IEEE Trans. Geosci. Remote Sens. **37**, 917–926 (1999).
17. A. Taflove and S. C. Hagness, *Computational Electrodynamics: The Finite-Difference Time-Domain Method* (Artech House, 2005).
18. S. D. Gedney and Z. Bo, “An auxiliary differential equation formulation for the complex-frequency shifted PML,” IEEE Trans. Antennas Propag. **58**, 838–847 (2010).
19. W. Choi, A. P. Mosk, Q. H. Park, and W. Choi, “Transmission eigenchannels in a disordered medium,” Phys. Rev. B **83**, 134207 (2011).